

O-Asn N distance is lengthened by about 0.8 Å. Figure 5 shows a stereo plot of the superimposed all-trans and cis bond containing structures after minimization. While the all-trans cyclic heptapeptide *cyclo*(Ala₇) conformation so generated may not be optimal, it illustrates that the two-turn β-bulge backbone is also accessible to cyclic heptapeptides in the absence of an *N*-alkyl residue.

Investigations of cyclic heptapeptide structures in three "phases" (solid, liquid, computer) suggest that the two-turn β-bulge motif is a stable, accessible one for several constitutional and conformational variants. This backbone may represent a useful addition

to the growing library of conformationally defined cyclic peptide backbones and thus be of utility in modeling interesting protein features as well as in the design of conformationally restricted pharmacological tools.

Registry No. 1, 25428-71-1; 1-4H₂O, 59953-96-7.

Supplementary Material Available: Tables of anisotropic thermal parameters for non-hydrogen atoms and hydrogen atom coordinates (7 pages); listing of structure factors (28 pages). Ordering information is given on any current masthead page.

Conformation of a Cyclic Heptapeptide in Solution: An NMR Constrained Distance Geometry Search Procedure

Catherine E. Peishoff,* John W. Bean, and Kenneth D. Kopple

Contribution from the Department of Physical and Structural Chemistry, SmithKline Beecham Pharmaceuticals, P.O. Box 1539, King of Prussia, Pennsylvania 19406.

Received November 8, 1990

Abstract: A constrained distance geometry search procedure was used in conjunction with proton NMR data to determine the conformation of the cyclic heptapeptide evolidine, *cyclo*(Ser-Phe-Leu-Pro-Val-Asn-Leu), in dimethyl sulfoxide solution. Key features of the search procedure included more even sampling of dihedral angle space, generation of many conformations, exclusion of electrostatic interactions in energy minimization steps, and evaluation of possible conformations by their prediction of experimental data. With use of this procedure, two classes of closely related backbone conformations were identified for the cyclic heptapeptide. Both are similar to the recently determined crystal structure which can be described as containing a β bulge flanked by two β turns. Inclusion of electrostatic interactions in the energy minimization steps did not result in different backbone conformations provided that the NMR derived distance constraints were included. This latter result confirms that incorporation of NMR derived distance constraints can be an effective means of including solvent and electrostatic interactions in the conformational calculations for compounds in this size range.

If cyclic oligopeptides are to be used as conformationally constrained molecules for identifying the biologically active conformations of peptides, the range of conformations accessible to them must be understood. A crystal structure, if obtained, indicates a possible, but not necessarily the only, conformation. In solution, multiple conformations are often possible and the conformation-determining information is limited to what is experimentally observable. In the past, suggested solution conformations have been based on consistency with the limited data, but a search for multiple conformations consistent with the observations has not been carried out. Molecular dynamics has been used to refine structures generated from NMR data, but molecular dynamics refinement will not generally result in a broad-ranging search for additional conformations consistent with the observations unless multiple, conformationally distinct starting points are tried.

We have recently reported a procedure using distance geometry to search conformation space of cyclic oligopeptides in the absence of experimental data.¹ Important features of this procedure include use of torsion angle sampling for 1,4 distances (introduced to maximize the breadth of the search) and exclusion of electrostatic interactions from energy minimization steps. With the inclusion of constraints derived from NMR observations, the same distance geometry search can be used to find the conformational possibilities that agree with experiment. This paper describes the incorporation of experimental data into that procedure as applied to a cyclic heptapeptide and also compares conformational results obtained by varying the procedure to include electrostatic effect as a way of ascertaining their importance to this type of search.

A crystal structure of the cyclic heptapeptide evolidine, *cyclo*(Ser-Phe-Leu-Pro-Val-Asn-Leu), was recently solved in this laboratory.² Some time ago, a probable solution conformation of evolidine was proposed on the basis of limited NMR observations (coupling constants, solvent, and temperature effects on chemical shifts).³ Although that proposed NMR structure has now turned out to be close to the crystal structure, it is based on more limited data than would be available today and other possibilities may not have been well considered. We have therefore reinvestigated the NMR spectra of evolidine to obtain quantitative nuclear Overhauser effect (NOE) data, in accord with current practice, and we have applied these NMR data to constraining a distance geometry based conformational search. The probable conformations identified by the search were further screened on the basis of predicted Overhauser interactions additional to the incorporated data.

Two main conclusions are reached from these studies, one in regard to the evolidine backbone and the other in regard to the search methodology: Incorporation of NMR constraints can be an effective means of including solvent and electrostatic interactions in a conformation search of molecules of this size. The probable cyclic heptapeptide backbone conformations in solution, two classes of which are identified, are very close to the conformation in the crystal. This supports the β-turn/β-bulge backbone as a generally probable cyclic heptapeptide conformation.²

Methods

A flowchart indicating the procedure used for generation and evaluation of evolidine solution conformations is given in Figure 1. Details

(1) Peishoff, C. E.; Dixon, J. S.; Kopple, K. D. *Biopolymers* 1990, 30, 45-56.

(2) Eggleston, D. S.; Baures, P. W.; Peishoff, C. E.; Kopple, K. D. *J. Am. Chem. Soc.*, preceding paper in this issue.

(3) Kopple, K. D. *Biopolymers* 1971, 10, 1139-1152.

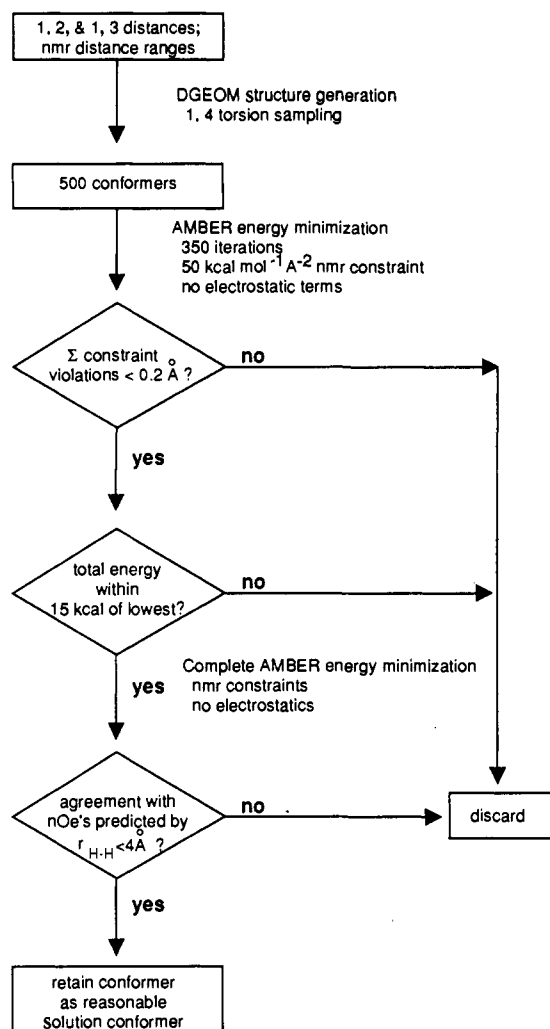


Figure 1. Flowchart illustrating the procedure used for the generation and evaluation of evolidine solution conformations.

of the individual steps are described under both the methods and results sections.

Proton Magnetic Resonance Experiments. An evolidine⁴ sample was prepared at a concentration of 33 mM in 0.5 mL of DMSO-*d*₆ (99.9 atom %, MSD Isotopes); 3 μL of tetramethylsilane was added as a chemical shift reference. All experiments were performed at 30 °C.

Proton magnetic resonance spectra were recorded at 500 MHz on a JEOL GX500 NMR instrument. P.E.COSY,⁵ TOCSY,^{6,7} and NOESY^{8,9} 2D NMR experiments were performed with a spectral width of 5000 Hz and 2048 complex points. In all experiments, the relaxation delay was set to be 5 times longer than the longest measured *T*₁ value. In the P.E.COSY experiment, the evolution time, *t*₁, was incremented for 512 steps. In the TOCSY and NOESY experiments, 300 *t*₁ values were collected. The TOCSY experiment was recorded with a mixing time of 60 ms. This was sufficient to observe proton-proton interactions at a distance up to and including five bond lengths. NOESY spectra were recorded with mixing times of 30, 60, 90, 120, 150, 180, 210, and 240 ms. The sample was not removed from the magnet between experiments.

NMR spectra were processed with use of the FTNMR software developed by Hare Research, Inc. For the P.E.COSY spectrum, a 30° shifted sine bell apodization function was applied along *t*₂ and a 30° sine bell apodization function was applied along *t*₁. Both domains were zero filled to 2048 real data points. The TOCSY spectrum was apodized with a 60° shifted sine bell in *t*₂ and a 60° sine bell in *t*₁ and zero filled to

Table I. Distance Constraints Derived from NOE Measurements for Evolidine in DMSO-*d*₆ at 30 °C

residue	proton	residue	proton	derived distance	lower bound	upper bound
Leu3	HN	Leu3	H α	2.81	2.53	3.20
Leu3	HN	Phe	H α	2.16	1.45 ^a	2.48
Leu7	HN	Asn	H β 1 ^c	2.37	2.14	2.73
Leu7	HN	Asn	H β 2 ^c	3.48	3.13	4.00
Leu7	HN	Leu7	H α	2.91	2.62	3.20
Leu7	HN	Asn	H α	2.51	2.26	2.88
Val	HN	Pro	H γ R	3.12	2.81	3.59
Val	HN	Asn	HN	2.21	1.99	2.54
Val	HN	Pro	H δ R	2.94	2.65	3.39
Val	HN	Leu3	H α	2.46	2.22	2.83
Ser	HN	Phe	HN	2.22	2.00	2.56
Ser	HN	Leu7	HN	2.34	2.11	2.69
Ser	HN	Leu7	H α	3.68	3.32	3.82
Asn	HN	Leu3	H α	2.51	2.26	2.89
Asn	HN	Asn	H β 1 ^c	2.95	2.66	3.40
Asn	HN	Asn	H β 2 ^c	2.87	2.58	3.30
Phe	HN	Phe	H β 2 ^c	3.70	3.33	4.25
Phe	HN	Phe	H β 1 ^c	2.87	2.59	3.30
Phe	HN	Ser	H α	3.97	3.57	3.82
Phe	H α	Phe	H β 1 ^c	180 ± 30°	3.06 ^b	3.11 ^b
Phe	H α	Phe	H β 2 ^c	60 ± 30°	2.35 ^b	2.73 ^b

^a Value set according to closest approach determined by the distance geometry algorithm. ^b Value determined from coupling constant data. ^c Numerals indicate distinguishable protons, but do not imply prochirality.

a 1024 × 1024 matrix. The NOESY spectra were apodized with a 90° sine bell squared function in both dimensions and zero filled to 1024 × 1024 matrices.

Proton chemical shift assignments were made according to standard procedures.¹⁰

Interproton distances were calculated from the integrated NOE crosspeak intensities of the 180-ms NOESY dataset with use of the FTNMR software and were calibrated by taking the proline β 1- β 2 NOE distance to be 1.75 Å (Table I). Interproton distances were also calculated from angles determined by $J_{\alpha\beta}$ coupling values according to the expression $J_{\alpha\beta} = 11.0 \cos^2 \theta - 1.4 \cos \theta + 1.6 \sin^2 \theta$.¹¹ Distance constraints were derived from these angles by calculating the distance between the H α and H β protons in a well-built residue at χ angles $\pm 30^\circ$ from the calculated angle value. Side chain atoms beyond C β (except for proline) are not likely to be constrained in a cyclic peptide of this size in solution, and data for them were not included in the search.

Conformation Generation. Five hundred conformations were generated for evolidine with use of the distance geometry program DGEOM,¹² modified to include torsion angle sampling for 1-4 atomic relationships and to exclude bounds correlation.¹ Input consisted of a geometrically well-built starting structure, i.e. having amino acid bond lengths and angles consistent with the crystallographic literature, of arbitrary conformation from which the program calculates the fixed 1,2 (bond) and 1,3 (angle) distances. All ϕ and ψ angles were considered fully rotatable, proline being limited only by its ring, and amide groups were constrained to be planar, but allowed to be either cis or trans. The constraints derived from the NMR NOE measurements were added as distance bounds between appropriate protons (Table I). Bounds ranging in size from 0.05 to 1 Å were calculated as -10% and +15% of the interproton distance derived from NOE measurements or from torsional angles as described above. The NOE-derived constraints used in structure generation were all those observed for which quantitative crosspeak volume estimates could be made. Excluded was one crosspeak (HN Val to H α of either Leu3 or Pro) for which spectral overlap precluded assignment (see Discussion). In the cases of 1,4 and 1,5 distances, the bounds were compared to those calculated from a geometrically well-built residue and adjusted when necessary to the limiting values derived by torsional rotation. This prevents selection of interatomic distances that are not physically attainable, thus increasing the efficiency of the search procedure. For those

(4) Studer, R. O.; Lergier, W. *Helv. Chim. Acta* **1965**, *48*, 460.

(5) Mueller, L. J. *J. Magn. Reson.* **1987**, *72*, 191-196.

(6) Levitt, M. H.; Freeman, R.; Frenkiel, T. J. *J. Magn. Reson.* **1982**, *47*, 328-330.

(7) Bax, A.; Davis, D. G. *J. Magn. Reson.* **1985**, *65*, 355-360.

(8) Macura, S.; Ernst, R. R. *Mol. Phys.* **1980**, *41*, 95-117.

(9) States, D. J.; Haberkorn, R. A.; Ruben, D. J. *J. Magn. Reson.* **1982**, *48*, 286-292.

(10) Wuthrich, K. *NMR of Proteins and Nucleic Acids*; John Wiley & Sons, Inc.: New York, 1986.

(11) Kopple, K. D.; Wiley, G. R.; Tauke, R. *Biopolymers* **1973**, *12*, 627-636.

(12) The DGEOM program was provided by J. Blaney, PROTOS, 6455 Christie Ave., Emeryville, CA 94608, and is available from QCPE, Department of Chemistry, Indiana University, Bloomington, Indiana 47405.

(13) Weiner, S. J.; Kollman, P. A.; Nguyen, D. T.; Case, D. A. *J. Comput. Chem.* **1986**, *7*, 230-252.

Table II. Proton Chemical Shifts of Evolidine in DMSO-*d*₆ at 30 °C^a

residue	HN	H α	H β	H γ	H δ	H ϵ	H ζ	J coupling
Ser	7.98 (7.81)	4.27	3.62/3.58					
Phe	7.37 (7.61)	4.43 (4.51)	2.95/2.62		7.14	7.21	7.24	$\alpha\beta_1 = 9.1$ Hz $\alpha\beta_2 = 3.9$ Hz
Leu3	8.89 (8.02)	4.23 (4.63)	1.57/1.19	1.76	0.87/0.82			$\alpha\beta_1 = 12.6$ Hz $\alpha\beta_2 = 2.6$ Hz
Pro		4.25 (4.08)	2.34 R/1.97 S (1.65/2.15)	1.84 S/1.49 R	3.43 S/3.23 R			
Val	8.20	3.70 (4.02)	2.25 (2.08)	0.96				
Asn	7.77	4.36 (4.48)	3.12/3.03		7.80/7.25			$\alpha\beta_1 = 3.6$ Hz $\alpha\beta_2 = 4.8$ Hz
Leu7	8.27 (7.83)	3.86	1.59/1.49	1.78	0.91/0.82			$\alpha\beta_1 = 12.2$ Hz $\alpha\beta_2 = 4.3$ Hz

^aProton chemical shifts of a minor conformer are given in parentheses. Coupling constants obtained from the P.E. COSY are listed.

distances for which the upper bound was adjusted, 0.2 Å was added to ensure that an anti orientation (180°) could be selected. For one very strong NOE value, the lower bound was allowed to be set by the DGEOM program with use of van der Waals radii which in that program are approximately 0.3 Å smaller than typical values. Prochirality could be determined for the β , γ , and δ protons of proline; therefore prochirality constraints were imposed at these carbons.

Conformation Evaluation. The conformers generated by the distance geometry algorithm were subjected to minimization using the program AMBER 3.0.¹⁵ The procedure starts with a 350-step minimization in the absence of electrostatic energy terms. The distance bounds described above were incorporated by using a flat-bottomed well potential with harmonic sides such that no penalty was assessed for distances within the bounds. A force constant of 50 kcal mol⁻¹ Å⁻² was used for each bounds pair. After all conformers had been minimized for 350 steps, the structures were ranked according to constraint energy, a term which describes the degree to which a conformer violates the NOE data. A cutoff of 2 kcal/mol was applied, which represents deviations from the constraints which could amount to a uniform 0.042 Å at one extreme or a maximum single deviation of 0.2 Å at the other. Only conformers below this cutoff value, 83 of the 500 structures, were considered further. These were reordered according to total energy, leaving 36 structures after a 15 kcal/mol total energy cutoff was applied. Finally, these 36 conformers were subjected to a complete minimization procedure with distance constraints applied throughout, again without electrostatic terms. A complete minimization is defined as either the norm of the gradient of the energy reaching 0.01 kcal/mol Å or 10 000 iterations. This number of iterations was determined to be more than sufficient to define the structure and settle the energy. These conformers were then reordered on total energy. As a test of conformational stability, these minimized structures were subjected to an additional 50 iterations, now with electrostatic terms and distance constraints, followed by 350 iterations with electrostatics and no distance constraints. As a contrast to the minimization procedure without charges, two additional independent minimizations were performed. In the first, the 36 conformers selected as described above were completely minimized with distance constraints and electrostatics applied throughout. In the second, the 36 conformers were completely minimized with electrostatics throughout, but with no distance constraints applied. When charges were present, a constant dielectric, $\epsilon = 1$, was used with a large (99 Å) non-bond cutoff so that all nonbond interactions are considered.

Results

Nuclear Magnetic Resonance Data. Proton chemical shift assignments and $J_{\alpha\beta}$ coupling values are given in Table II. It was possible to make prochiral assignments of the proline side chain methylene protons on the basis of relative interproton NOE intensities. The proline H α had a stronger NOE to one H β , assigned *pro-S*, than to the other H β , assigned *pro-R*. Observations of the relative NOE intensities of each H β to each H γ and, in turn, each H γ to each H δ permitted complete prochiral assignment of that side chain. Proton chemical shifts of a minor conformer in slow exchange were assigned from observed chemical exchange crosspeaks. These exchange crosspeaks were of the same sign as those observed between dipolar-coupled spins, negative NOE, but were distinguished from the latter on the basis of signal intensity of resonances in the one-dimensional proton magnetic resonance spectrum. Resonances arising from the minor conformer had less than 5% the signal intensity of those of the major con-

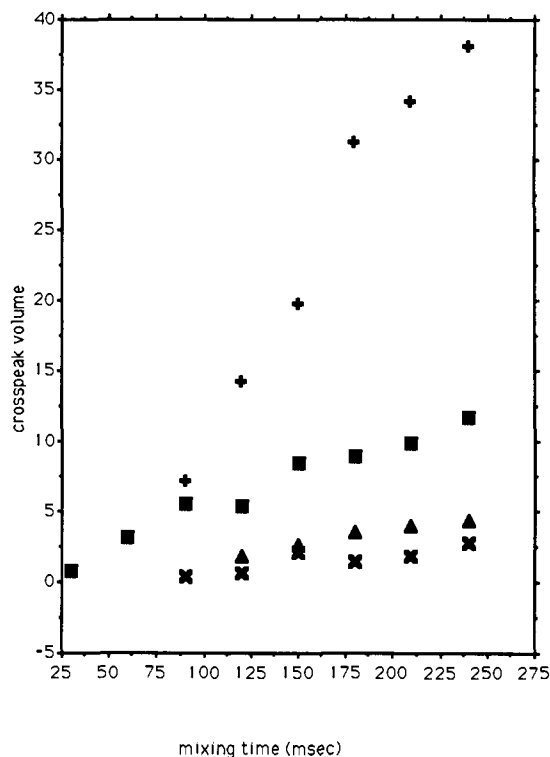


Figure 2. Representative NOE buildup curves. The fixed distance (1.75 Å) between proline H β R and H β S (+) was used to calibrate all other crosspeak intensities. HN of Leu3 to H α of Phe (■) represents a short amide- α interproton distance; HN of Leu7 to H α of Leu7 (▲) represents a long amide- α interproton distance; and HN of Asn to H α of Leu3 is a cross ring NOE (×). NOE volumes at 180 ms mixing time were used to calculate the distance constraints.

former. Representative NOE buildup curves are shown in Figure 2. Proton-proton NOE's for a peptide of this size in DMSO are relatively small (the crosspeak volume for the proline H β -H β interaction is about 10% of the diagonal peak volume at 180 ms) and the NOE data were relatively noisy. Some weaker NOE's were not reliably observed at mixing times less than 120–150 ms, so that it was impractical to use initial buildup rates to calculate constraint distances. Constraint distances were instead calculated from peak volumes at 180 ms. Where sufficient data were available, constraints were also calculated from slopes and at poorest agreement were within 15%, and generally within 10%, of those obtained from the 180 ms data set.

Search Results. The results of the constrained conformational search can be summarized in a series of Ramachandran plots, one for each residue (Figure 3). These are shown for the 36 selected conformers as minimized without electrostatics. While most of the maps show populations in one major region, with the exception of the proline map they also indicate alternative residue conformations consistent with the applied experimental distance con-

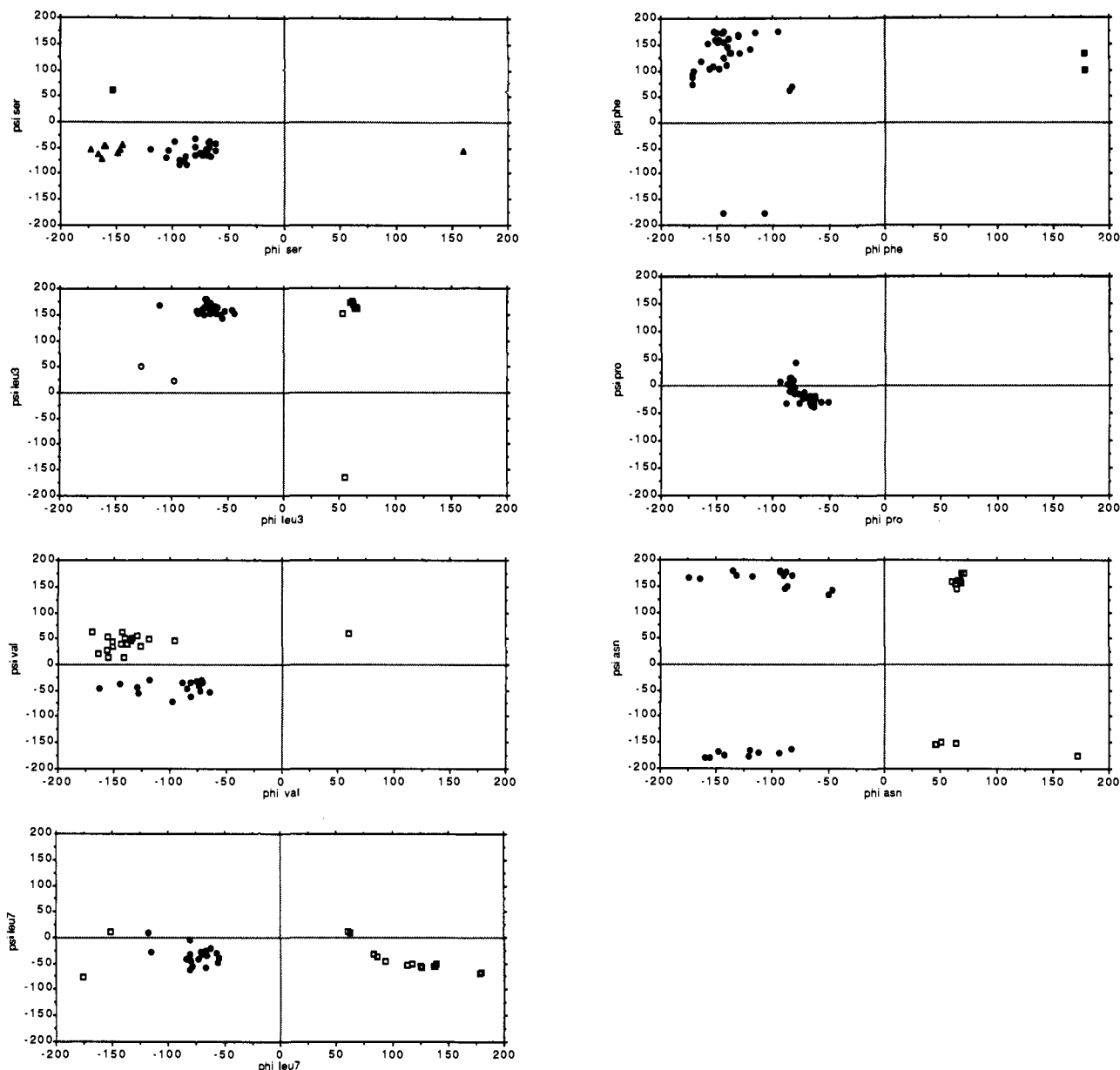


Figure 3. Ramachandran plots depicting dihedral variation in the 36 conformers fully minimized with distance constraints, but in the absence of electrostatic interactions. See text for an explanation of the symbols.

straints. It is clear that more than one solution can be obtained given the experimental data used, and it is important to consider the alternative conformations in the light of both quantitative and qualitative experimental data before suggesting any most probable solution conformer(s). At this point in a search procedure, total energy considerations are often introduced. However while energy terms are important, choosing a best fit conformation only on the basis of calculated energy alone may say more about the minimization method than the agreement with experiment. Further use of the experimental observations may be made by calculating the interproton distances predicted by each of the (36) likely conformers. These interproton distances provide criteria additional to the originally selected quantifiable NOE observations, which may be used to exclude particular conformers as major contributors to the experimental sample:

(1) Are there NOE's that should be observed, but are not? In the present work, interproton distances up to 4 Å involving backbone protons in major conformers give rise to observable Overhauser crosspeaks at the 180 ms mixing time (Table I).

(2) Are there NOE's that should not be observed, but are? In the present work, with one exception because of ambiguous assignment, all of the observed NOE's were utilized in the original conformation search.

(3) Are the relative intensities of predicted and observed NOE's consistent? A conformation that predicts, for example, that HN to glycine H α pairs should have similar intensities when they are experimentally different is suspect. In the present case, most of the criteria in this category, but not all, will have been included in the original set of distance constraints.

The plots in Figure 3 are descriptive of both the overall search results and the calculation screen just described. Each point represents a dihedral angle found in one of the 36 conformations. Because there is not a wide range of conformational variability, angles can be grouped to indicate those in backbone conformations allowed by the constraining NOE data that pass the screens listed above (solid symbols). Angles that are allowed by the input NOE data but that predict data violations on calculation of interatomic distances are indicated by open symbols. Variations in the symbols are used to indicate clusters of angles which are indicative of the conformational variation.

The 36 conformers can be categorized into four groups: (1) structures consistent with the crystal structure; (2) geometric isomers differing from the crystal in peptide bond isomerism; (3) structures containing amide plane rotations different from the crystal; and (4) structures with a Pro-Val twist leading to an orientation of the proline that is more perpendicular to the

Table III. Analysis of *cyclo*(Ser-Phe-Leu-Pro-Val-Asn-Leu) Conformations

<i>E</i> , kcal/mol	rms ^a	Ser		Phe		Leu3		Pro		Val		Asn		Leu7	
		ϕ	ψ	ϕ	ψ	ϕ	ψ	ϕ	ψ	ϕ	ψ	ϕ	ψ	ϕ	ψ
crystal	0.00	-100	1	-157	74	-65	151	-92	13	-95	-16	-159	150	-53	-30
min A ^b															
set a 3.44 (-179.58)	0.43	-62	-40	-142	109	-76	156	-85	-4	-77	-34	-138	-170	-90	-39
set b 3.93 (-183.86)	0.59	-71	-54	-90	60	-62	149	-84	-1	-74	-54	-106	-166	-83	-53
set a 6.82 (-176.02)	0.52	-68	-47	-139	106	-71	148	-88	6	-73	-47	-146	-169	-81	-23
set b 9.15 (-158.79)	0.75	-73	-59	-90	65	-60	157	-77	-22	-85	-48	-84	174	-73	-56
set a 9.60 (-171.77)	0.58	-67	-45	-148	106	-66	150	-85	7	-75	-47	-152	-170	-78	-22
min B ^c															
-191.34	0.53	-66	-64	-82	61	-59	142	-85	-2	-85	-14	-152	-177	-66	-50
-178.60	0.70	-64	-33	-165	101	-63	148	-85	6	-69	-47	-164	-175	-60	-24
min C ^d															
-180.62	0.79	156	-69	-77	69	-61	153	-76	-30	-58	-36	-129	149	-72	76

^aRoot-mean-square deviation of ring atoms N, C α , C and directly attached atoms O and C β from corresponding atoms in the crystal structure. ^bTotal energy for full minimization without electrostatics and with distance constraints applied throughout. The number in parentheses is the total energy after an additional 50 steps with electrostatics and distance constraints applied. ^cTotal energy for full minimization with electrostatics and distance constraints applied throughout. See text. ^dTotal energy for full minimization with electrostatics and without distance constraints applied. See text.

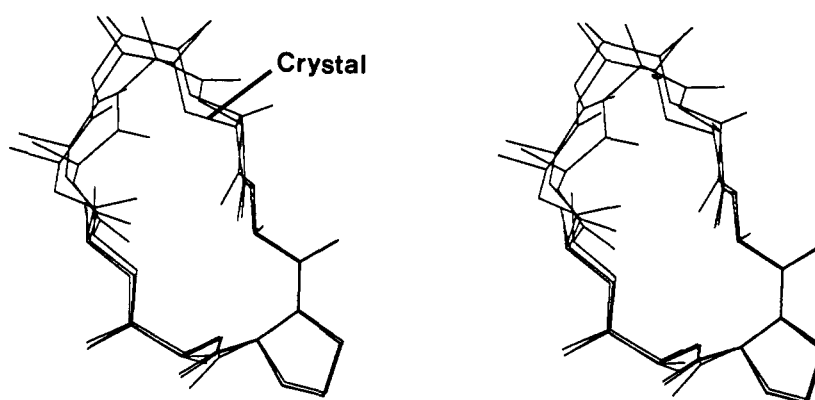


Figure 4. Stereo plot illustrating the two solution conformers overlaid on the crystal structure such that the backbone atoms in Leu3, Pro, and Val are superimposed. Except for proline, side chain atoms beyond β are omitted.

backbone plane than that in the crystal. Many of the conformers have features of more than one category. Of these four categories, only conformers consistent with the crystal structure obey all the observed experimental data.

The geometric isomers include conformers containing either a *cis*-Val-Asn or *cis*-Ser-Phe peptide bond in addition to the *cis*-Leu3-Pro peptide bond. There is also an all-trans variant. The *cis*-Val-Asn and *cis*-Ser-Phe conformers predict distances less than 3.0 Å for the HN_{*i*} to H α_{i+1} protons of the two residues, but the corresponding NOE's which should be very strong are not observed experimentally. The all-trans conformer predicts NOE's between the Leu3 HN and both δ protons of proline (2.94 and 3.26 Å); these also are not observed.

Single amide plane rotational isomers were found for Asn-Leu7 and Val-Asn, and coupled amide plane rotations were found for Ser-Phe-Leu3 and Asn-Leu7-Ser. The Asn-Leu7 rotation predicts an NOE between H α of Asn and HN of Ser (3.6 Å) which is not observed. Similarly, the Val-Asn rotation predicts an NOE for H α of Leu3 to H α (3.5 Å) of Asn which is also not observed. The coupled rotations predict cross-ring NOE's. The Ser-Phe-Leu3 rotations indicate an observable distance between either Leu3 HN to Asn HN or Phe HN to Leu7 HN. The Asn-Leu7-Ser rotations predict Asn H α to Phe HN or to Ser HN, or Asn HN to Ser HN or to Phe HN. In both cases, the predicted interproton distances are less than 3.7 Å, but NOE's are not experimentally observed.

Structures containing the perpendicular proline ring (category 4) suggest an NOE between the α protons of Leu3 and Val with distances less than 3.5 Å. This is also not observed.

Of the 36 conformers, 31 can be ruled out on the basis of the backbone NOE's they predict even though they obey the constraints derived from observed NOE's and can be considered low in energy.

The remaining 5 structures are listed by energy with their dihedral angles in Table III under the heading min A. They can be placed into two sets on the basis of dihedral similarity and these are indicated as a or b. An overlay of the lowest energy conformer from each of the sets is shown with the crystal structure as a stereo pair in Figure 4. For discussion purposes, the dihedral angles for the lowest energy conformer obtained from the set of 36 minimized *with electrostatics and distance constraints applied throughout* are listed in Table III (min B). Also included are the angles for the conformer from the set minimized *with electrostatics, but without distance constraints* that most closely resembles the crystal structure (min C). This structure is the fifth lowest in energy in the set.

Discussion

Probable Solution Conformation. Two sets of low-energy conformations (a and b, Table III) can be identified for evolidine. As seen in Figure 4, they are related to each other by what may be described as a hinge motion about an axis passing through the C α carbons of phenylalanine and asparagine. This may or may not be indicative of the solution dynamics of the peptide. Both conformations obey all the observable NMR data without predicting additional data, as does the crystal structure reported in the companion paper.² The crystal structure may be used as a reference point in evaluating conformations generated during the various minimization procedures, and root-mean-square deviations from the crystal structure are reported for the backbone atoms, carbonyl oxygens, and β -carbons of the conformers in Table III. For the unexcluded conformers obtained by minimization without electrostatics, but with distance constraints, no conformer differs from the crystal structure by a root mean square greater than 0.75 Å, with a low value of 0.43 Å. This is indicative of a peptide which

predominantly populates a small region of conformational space. As a test of their conformational stability, these conformers were additionally minimized in the presence of electrostatic interactions for 50 iterations with distance constraints, followed by 350 iterations with electrostatics, but without the distance constraints. None of the 5 conformers changed as a result of these additional 400 steps by greater than 0.32 Å root-mean-square deviation in the positions of the backbone atoms, the carbonyl oxygen, and C β . While a 39° difference was the maximum for any one dihedral angle, most differences were less than 15°. This would suggest that while the distance constraints are integral to the minimization path, the minimized structures are stable in their own right and not held in place by the constraints. In other words, the electrostatic interactions are implicit in the NMR data. Greater variation would be expected if the NMR data reflected conformational averaging over widely differing conformations because consistent electrostatic interactions would not necessarily arise in a "virtual" conformation. Conformational stability is also supported by the results of the minimizations that included both electrostatics and distance constraints throughout. Low-energy solutions very similar to those in Figure 4 are identified (see Table III, min B). However these low-energy structures are not descended from the same members of the original set of 36 as are the low-energy structures obtained without electrostatic terms. This affirms a unique solution to the NMR data in that, so long as the NMR data are applied, the same solution is arrived at regardless of the influence of electrostatics on the minimization path. Electrostatic terms are known to be quite substantial in determining minimum energy structures. The assumption that NOE constraints are an effective way of including the effects of solvent in a conformational search, as has been shown in a molecular dynamics simulation of vancomycin,¹⁴ is also supported for molecules of this size.

One additional question to be considered is the effect of maintaining distance constraints throughout the calculations. It has been suggested for an enkephalin analogue¹⁵ that using the constraints in the structure generation step only is sufficient. For evolidine, a complete minimization was also performed on the 36 conformers selected as previously described with full electrostatics and no distance constraints. These starting structures were already more probable than any random selection of 36 from the initial 500, in that they were chosen under both energy and distance constraint guidelines and thus should have a higher probability of leading to a conformer which obeys the distance constraints. Despite this, the closest root-mean-square fit to the crystal produced by this electrostatics only minimization is 0.79 Å, with the variation occurring predominantly in an amide plane rotation between Leu7 and Ser. This rotation, however, produces predicted NOE's that are inconsistent with the experimental data. The Ser HN to Leu7 HN and H α are predicted to have distances of 3.79 and 2.33 Å, respectively, while the experimentally derived distance bounds are 2.11–2.69 and 3.32–3.82 Å, respectively. This particular amide plane rotation, then, is inconsistent with the experimental data. This conformer is listed in Table III as min C. Dihedral angle plots, like those in Figure 3, for these solutions show a much higher degree of scatter as compared to the results in Figure 3, and these conformers show a greater degree of violation of the distance constraints. Minimization in this fashion would appear to be much more dependent on the sampling procedure and would require a large sample set to have any confidence in finding a reasonable solution. It has been previously shown¹ that in a sample size of 500 generated with no distance constraints the crystal conformation of evolidine was not found. The current

results would indicate that this sample size is sufficient only if the NMR data are applied throughout the structure generation and minimization procedure. Alternatively, a cyclic peptide for which there is a more limited number of conformations available, which may be the case for the cyclic enkephalins, may produce experimentally valid structures even without distance constraints.

Methodology Considerations. Two points related to methodology deserve further clarification and/or emphasis. The first concerns the choice of distance bounds. A single interproton distance is calculated from an observed NOE but, even in molecules that can be considered conformationally stable overall, the NOE's must reflect some internal mobility. Since the NOE's are proportional to $\sum p_n r_n^{-6}$ (p_n = fractional population of conformation n , r_n = corresponding interproton distance), the derived interproton distances will be weighted toward closest approaches. Whether or not there is experimental error, a set of single values for each NOE-derived distance thus would not be likely to produce reasonable three-dimensional structures. Ranges of allowed interproton distances from which to choose each trial distance are therefore appropriate. The bounds used in this work were kept narrow enough (–10%, +15%) to reduce the chance of producing conformations that would violate the experimental data yet allow room for construction of multiple three-dimensional conformations. In testing for appropriate bounds, it was found that leniency on the upper side of the distances calculated from the NOE crosspeak volumes was more productive of three-dimensional solutions than leniency on the lower side. This is consistent with the NOE-derived distances being weighted toward small values. Selecting too many distances from the lower side of the calculated distance also leads to conformers with bad van der Waals interactions.

A second issue is the choice of force constant with which to constrain the distance geometry structures within the NOE-derived bounds during energy minimization steps. This choice can dictate the minimization path. In choosing a force constant for the distance constraints it is important to balance between obeying the constraints and maintaining reasonable geometries, particularly if the distance constraints are to be maintained throughout the calculations. In the AMBER parameter set, force constants are generally in the range of several hundred kcal mol⁻¹ Å⁻² for bonds, and for angles under 100 kcal mol⁻¹ rad⁻². A force constant of 50 kcal mol⁻¹ Å⁻², used in this work, is not strong enough to alter bonds, but it will compete against most angles. If the experimental data set is good, i.e. representative of one conformation or several closely related conformations, then resulting structures should have both good geometries and low violations of imposed distances. If the data set is too restrictive or represents more than one conformation, a combination of bad geometries and higher distance violations should arise. With a lower force constant for the NOE-derived constraints, the conformation selection will be more random. With a higher force constant, it is easier to develop bad geometries that obey the experimental data. It is possible to check the choice of constraining force constant and that the data set reflects a unique solution by performing a final minimization step without constraints and without electrostatic interactions, to determine the stability of the constrained solutions. This test was in effect carried out for the models in Table III, as described in the discussion above.

Conclusions

Taken together, the X-ray crystal structure,² the apparent solvent independence of conformation,³ and the internal consistency of the NOE data with a very limited range of backbone structures indicate that the β -turn/ β -bulge conformation of *cyclo*(Ser-Phe-Leu-Pro-Val-Asn-Leu) is a stable one. The distance geometry search protocol described here, in which experimental data are relied on for incorporation of electrostatic interactions as well as solvent effects, has been shown to be effective for solving conformations of cyclic peptides in this size range.

(14) Molinari, H.; Pastore, A.; Lian, L.; Hawkes, G. E.; Sales, K. *Biochemistry* **1990**, *29*, 2271–2277.

(15) Mosberg, H. I.; Sobczyk-Kojiro, K.; Subramanian, P.; Crippen, G. M.; Ramalingam, K.; Woodard, R. W. *J. Am. Chem. Soc.* **1990**, *112*, 822–829.